

NUMERICAL STUDY OF PRESSURE DROP IN THE HORIZONTAL SPIRALLY COILED TUBES

Omid SEYEDASHRAF

Department of Civil Engineering, Kermanshah University of Technology,
67178 Pardis St., Kermanshah, Iran.
o.seyedashraf@kut.ac.ir

Abstract: Flow characteristics of spirally coiled tubes in terms of their secondary flow and pressure drop are investigated. Four spirally coiled tubes with different curvature ratios; under constant wall temperature, are numerically simulated. In the system, water is entering the innermost turn and flows out at the outermost turn. To build the numerical model, a finite volume method with an unstructured grid system is employed for solving the Navier-Stokes equations system. Correspondingly, the standard $k-\epsilon$ turbulence model is employed to predict the flow development. Here, the mass flow rate in the spirally coiled tube is set to vary within the range 0.03-0.12 kg/s. The numerically obtained data of the pressure drop in the spiral coils are put side by side the experimental data reported in the literature. A close agreement is observed between the experimental data and the results of this study. Based on the results, a new correlation is proposed for predicting the pressure drop in horizontal spiral coils.

Keywords: Coil, Spirally Coiled Tube, Pressure Drop, Finite Volume Method, Standard $k-\epsilon$

INTRODUCTION

Spiral coils are regularly used curved tubes, which have been utilized in a wide variety of engineering applications such as heating, refrigerating systems, HVAC systems, steam generator and condensers in power plants and chemical reactors. In a curved tube, because of the differences between the inertial and centrifugal forces, a secondary flow originates in the cross section of the pipe. The heat transfer and flow developments in these tubes significantly depend on the performance of the induced secondary flow.

Flow and heat transfer in spiral pipes with circular or rectangular cross-section has been a topic of important fundamental engineering interests during the past decades. Orlov and Tselishchev (1964), illustrated an experimental research on heat transfer from spiral and helical coils with a turbulent water flow. They proposed a correlation to predict the inside heat transfer coefficient of spiral coils.

Ho et al. (1995 & 1999) employed correlations of the tube-side and air-side heat transfer coefficients to define the thermal functioning of the spiral-coil heat exchanger under cooling and dehumidifying conditions. Experimental benchmarks were evaluated to verify the results. Nakayama et al. (2000), studied the cooling potentialities of a fluid fluxing through a spiral coil, which was drowned in a cold water container. Accordingly, an axisymmetric mathematical scheme was invented and proposed to assess the temperature of the fluid in a spiral coil and that of the surface of the coil. Naphon and Wongwises (2002), reported an experimental survey on in-tube convective heat transfer coefficients in a spiral coil heat exchanger. The heat exchanger was made of six layers of homocentric spirally coiled tubes, each with five turns. The ef-

fects of relevant parameters were investigated. They proposed a novel formula based on their experimental data to simulate and predict in-tube heat transfer coefficient of spiral coils. Naphon and Wongwises (2003 & 2005), modified the mathematical model of Ho et al. (1995), by considering the fin efficiency and using the other accessible heat transfer coefficient correlations to prescribe the flow characteristics and heat transfer attributes of spiral coil tube heat exchanger subjected to wet-surface environment. The relevant parameters on the performance of the heat exchanger were discussed.

Naphon and Suwagrai (2007), experimentally and numerically investigated the heat transfer and flow developments in the horizontal spirally coiled tubes. They compared the heat transfer and pressure drop of a spirally coiled tube side by side those from the straight ones and compared them. It was revealed that because of the existence of centrifugal force, the pressure drop and Nusselt number acquired from the spirally coiled tube were 1.49, 1.50 times higher than the ones obtained from the straight tube, respectively. Mittal et al. (2009), using a mathematical model investigated the adiabatic flow of a refrigerant fluid through a spiral capillary tube making use of a homogenous model together with the metastable liquid. Lee et al. (2010), considered the air-side heat transfer properties of spiral-type circular fin-tube heat exchangers used as evaporators in household refrigerators. Moreover, Yoo et al. (2012), numerically investigated the flow characteristics of spirally coiled tubes making use of the state of the art Fluent CFD package. Different geometries with various Reynolds numbers were evaluated and was concluded that the Reynolds number following with the Nusselt number and friction factor have a stronger

effect compared to the curvature ratio of the spirally coiled tubes.

Though some investigations have been performed on performance and in-tube heat transfer of spiral coils, no thorough work has been reported on the pressure drop. The objective of this study is to obtain a correlation to determine the pressure drop for the steady state flow in horizontal spiral coils.

GEOMETRY OF SPIRALLY COILED TUBES

A scheme of a typical spirally coiled tube is presented in Figure 1. In this figure, b is the coil pitch and R_{min} and R_{max} are the minimum and maximum curvature radii, respectively. The curvature radius of a spiral coil, R_c , is defined as:

$$R_c = \frac{R_{min} + R_{max}}{2} \quad (1)$$

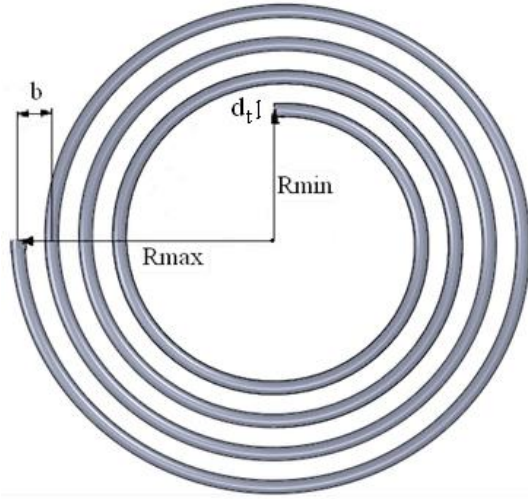


Figure 1. Schematic of a spiral coil

The geometrical specifications of the four coils that were used in the numerical study are given in Table 1.

Table 1. Coil Dimensions

Coil	R_{max} (mm)	R_{min} (mm)	d_t (mm)	b (mm)
1	250	100	10	50
2	200	125	10	25
3	172	82	8.025	18
4	136	82	8.025	18

MODEL DESCRIPTION

Governing Equations

The standard k - ε model is utilized to simulate the turbulent flow and heat transfer developments. Here, the governing equations are based on the conservation of mass, momentum, and energy. A state of the art CFD code is employed, which uses the finite volume method to transfer the continuous

equations into discretized ones by integration of the governing equation over the control volumes and eventually solve the linearized equations. The governing equations are defined as:

$$\frac{\partial(\rho)}{\partial t} + \frac{\partial(\rho u_i)}{\partial x_i} = 0 \quad (2)$$

$$\frac{\partial(\rho u_i)}{\partial t} + \frac{\partial(\rho u_i u_j)}{\partial x_j} = \frac{\partial \tau_{ij}}{\partial x_j} - \frac{\partial p}{\partial x_i} \quad (3)$$

$$\frac{\partial(\rho E)}{\partial t} + \frac{\partial(\rho u_j E)}{\partial x_j} = \frac{\partial}{\partial x_j} \left(k \frac{\partial T}{\partial x_j} \right) + \frac{\partial(\tau_{ij} u_j)}{\partial x_j} \quad (4)$$

where t is time, u_i is the i -th component of the Reynolds averaged velocity, x_i the i -th axis (with the axis x_3 vertical and oriented upward), ρ is the water density, P is the Reynolds averaged pressure and g is the acceleration due to gravity.

In a Newtonian fluid τ_{ij} is calculated as follows:

$$\tau_{ij} = \mu \left[\left(\frac{\partial u_i}{\partial x_j} + \frac{\partial u_j}{\partial x_i} \right) - \frac{2}{3} \frac{\partial u_k}{\partial x_k} \right] \quad (5)$$

The non-equilibrium wall-function treatment was adopted and the standard k - ε turbulence model, as the most robust, economical, reasonably accurate and long accumulated performance data, was included in the equations system.

The turbulent kinetic energy k , and the turbulent kinetic energy dissipation ε , are coupled to the main governing equations via the turbulent viscosity relation. Here, the equation for k contains additional turbulent fluctuation terms that are unidentified. Using the bossiness assumption, these fluctuation terms can be linked to the mean flow.

$$\frac{\partial(\rho k)}{\partial t} + \text{div}(\rho k \mathbf{U}) = \text{div} \left[\frac{\mu_t}{\sigma_k} \text{grad } k \right] + 2\mu_t E_{ij} \cdot E_{ij} - \rho \varepsilon \quad (6)$$

$$\frac{\partial(\rho \varepsilon)}{\partial t} + \text{div}(\rho \varepsilon \mathbf{U}) = \text{div} \left[\frac{\mu_t}{\sigma_\varepsilon} \text{grad } \varepsilon \right] + C_{1\varepsilon} \frac{\varepsilon}{k} 2\mu_t E_{ij} \cdot E_{ij} - C_{2\varepsilon} \rho \frac{\varepsilon^2}{k} \quad (7)$$

where U is the velocity vector, E_{ij} is the mean rate of deformation tensor, $C_{1\varepsilon}$ and $C_{2\varepsilon}$ are constants, and typical values of 1.44 and 1.92 are used. In these equations, the Prandtl number σ_k connects the diffusivity of k to the eddy viscosity and normally a value of 1.0 is used. Moreover, the Prandtl number σ_ε connects the diffusivity of ε to the eddy

viscosity and generally a value of 1.30 is used (Seyedashraf and Akhtari, 2016).

Boundary Conditions

The boundary conditions implemented in this study are as follows: the water inlet is defined as velocity-inlet, outflow boundary conditions are used to model the flow exit; since the details of the flow velocity and pressure are not known prior to solution of the flow problem. Additionally, the no-slip wall boundary condition in conjunction with a constant wall temperature T_w , as the thermal boundary condition was imposed on the spirally coiled tube wall.

Initial Conditions

At the inlet boundary condition, the uniform profiles of all the properties are considered, as follows:

$$u = u_{in}, v = 0, w = 0, k = k_{in}, \varepsilon = \varepsilon_{in} \quad (8)$$

The turbulent kinetic energy k_{in} , and the turbulent kinetic energy dissipation ε_{in} , at the inlet section are approximated from the turbulent intensity I , and a turbulent characteristics length L , as follows:

$$k_{in} = \frac{3}{2} (u_{in} I)^2, \quad \varepsilon_{in} = \frac{C_\mu^{3/4} k_{in}^{3/2}}{L} \quad (9)$$

The turbulence characteristic length L , is set to $0.07r$ (Versteeg and Malalasekera, 1995).

Numerical Modeling

The three-dimensional flow domain was divided into numbers of non-overlapping unstructured mesh with 505112 hexahedral segments and 527175 nodes. Out of different possible meshing schemes, the chosen form is suitable for both accuracy and the time duration of the convergence. The unstructured non-uniform grid system is shown in Figure 2.

The employed CFD code uses the finite volume method in conjunction with a coupling technique, which simultaneously discretizes and solves transport equations in the whole domain through a false time-step algorithm. Convection terms are linearized using third order monotone upstream centered scheme for conservation law (MUSCL) (Van Leer, 1976). The linearized system of equations is preconditioned in order to reduce eigen-values to the same order of magnitude. Pressure-implicit with splitting of operators (PISO) method was employed to deal with the problem of velocity and pressure coupling (Oliveira and Issa, 2001). PISO methods incorporate pressure effect through momentum equations into the continuity equation to obtain correction equations for pressure.

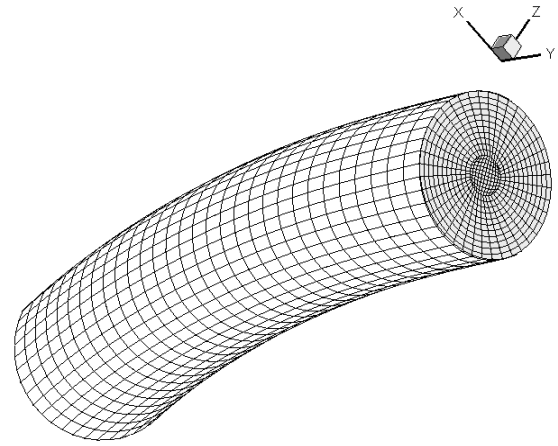


Figure 1. Grid form used to perform the computations.

2500 iterations for each simulation was reached in this study for a full convergence. The unstructured grid approach here has significantly enhanced the speed of convergence.

The conditions that were used in numerical study are given in Table 2.

Table 2. Employed variables in the CFD analysis

Variable	Range
Inlet water temperature, K	293
Wall temperature, K	320
Water flow rate, kg/s	0.03-0.12

RESULTS AND DISCUSSION

A numerical study for flow fields was conducted on a horizontal spiral coil, using water as the working fluid. Comparing the numerically obtained results it was concluded that the finite volume method in conjunction with the standard k- ε turbulence model has the capability of capturing specific flow behaviors in spiral coils. Figure 3 shows the development of axial velocity at different cross-sections ($\varphi = 90^\circ, 180^\circ, 360^\circ, 720^\circ$) for coil #1 at $Re = 38500$. As depicted in this figure, when the axial distance is small, the secondary flow would become weak. Due to the effect of centrifugal forces, the flow in the core of the pipe begins to be forced to the outer section of the bend. Moreover, as the φ parameter increases, the secondary velocity enhances and the high axial velocity zone shifts to the outer side, as shown in this figure.

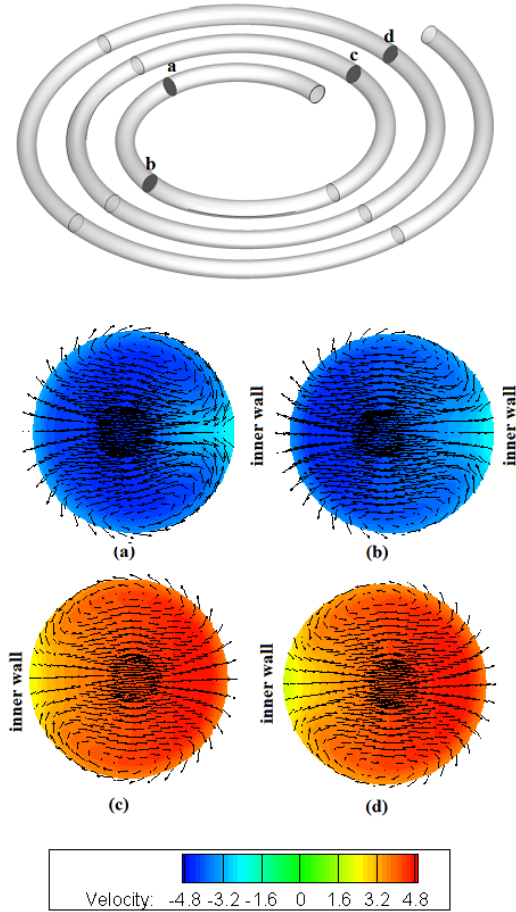


Figure 3. Velocity fields and vectors of water flow in a spirally coiled tube and different sections: (a) $\phi=90^\circ$, (b) $\phi=180^\circ$, (c) $\phi=360^\circ$, (d) $\phi=720^\circ$

Accordingly, the form of the secondary flow would depend on the axial distance from the inlet section. Figure 4 demonstrates the longitudinal pressure contours along the tube.

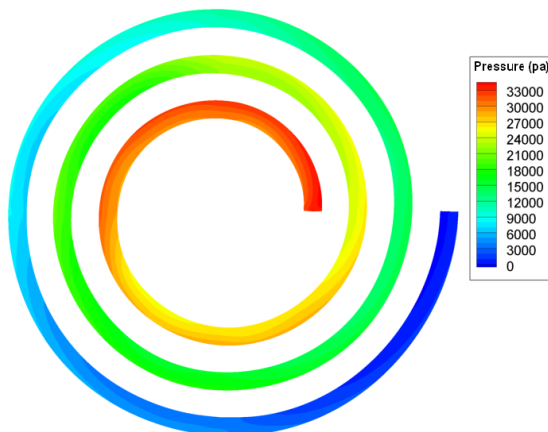


Figure 4. Pressure contours (pa).

Analysis of the Numerical Data

For flow in spiral coils, pressure drop ΔP , as a dependent variable, depends on the independent variables of the fluid properties (ρ and μ), the inlet velocity (u), and the parameters of the coil geometry (R_{\min} , R_{\max} , b , d_i). Thus:

$$\Delta P = f(\rho, \mu, u, R_{\min}, R_{\max}, b, d_i) \quad (10)$$

To obtain a correlation for pressure drop in spiral coils the form $EuG = \alpha Re^\beta$, which is the same form as that of Hagen–Poiseuille law $Eu(d/L)=16/Re$, and Blasius resistance law $Eu(d/L)=0.0791Re^{-0.25}$, has been used. Where $Eu = \Delta P / (0.5\rho u^2)$ is the Euler number and G is some geometrical dimensionless group, which depends on the geometry of the coil. This form of correlation has been used by some researchers for pressure drop in helical and spiral coils (Shaukat and Seshadri, 1971, Shaukat and Zaidi, 1979, Srinivasan, et al. 1968, Ramana and Sadasivudu, 1974, Dyke, 1978).

Shaukat (2001) developed a correlation for pressure drop in helical coil tubes, as follows:

$$EuGrhc = 0.09Re^{-1/5}, \quad Re > 1000 \quad (11)$$

where $Grhc$ is an appropriate geometrical parameter of helical coil.

Since the flow patterns; due to secondary flow of spiral coils are similar to those of helical coils, in this study, the pressure drop predicting correlation is considered as follow:

$$EuG = Re^{-1/5}$$

in which the power of Reynolds number is considered to be similar to the correlation of Shaukat (2001). In Eq. (12) the geometrical dimensionless parameter G , must be defined for a spiral coil.

Based on the numerical results attempts were made to obtain the best correlation for G , resulted in a relationship as follows:

$$G = 0.007 \left(\frac{R_{\max} + R_{\min}}{R_{\max} - R_{\min}} \right)^{-0.757} \left(\frac{d_i}{b} \right)^{-1.252} \quad (13)$$

Therefore, Eq. (12) can be written as:

$$Eu \left[\left(\frac{R_{\max} + R_{\min}}{R_{\max} - R_{\min}} \right)^{-0.757} \left(\frac{d_i}{b} \right)^{-1.252} \right] = 142.86 Re^{-1/5} \quad (14)$$

$$7000 < Re < 17000$$

The predicted results for pressure drop in horizontal spiral coiled tubes are compared with the experimental data presented by Naphon and Suwagrai (2007). Figure 5 indicates the computed pressure drop against the respective experimental values.

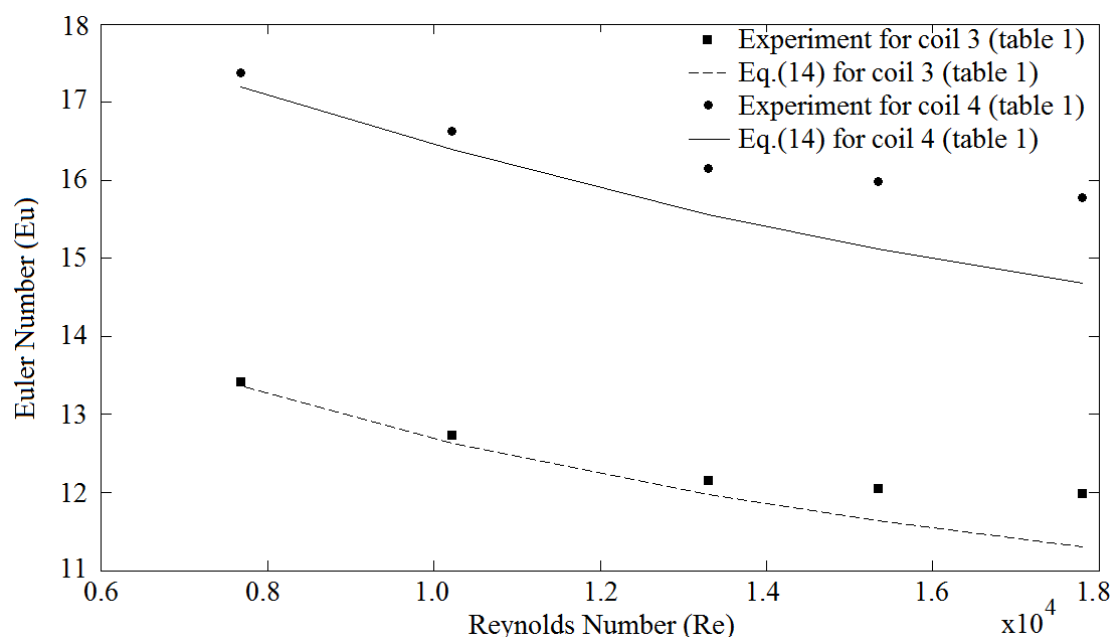


Figure 5. The Euler number computed by CFD (Eq. 14) against the experimental values of Naphon and Suwagrai (2007).

As it can be observed from the figure, there is a reasonable agreement between the numerical and experimental values. The largest discrepancies are obtained for the large mass flow rates, corresponding to the largest Reynolds number. The average and maximum deviations of Eq. (14) with the experimental data for the coil 3 and 4 (Table 1) are 6.27% and 11.05% respectively.

REFERENCES

1. Dyke, M.V., Extended Stokes series laminarflow through a loosely coiled pipe, *Journal of Fluid Mechanics*, 86(1): p. 129–145, 1978.
2. Ho J.C., Wijesundera, N.E., and S. Rajasekar, An unmixed-air flow model of a spiral cooling dehumidifying heat transfer. *Applied Thermal Engineering*, 19(8): p. 865–883, 1999.
3. Ho, J.C., Wijesundera, N.E., Rajasekar, S., and T.T. Chandratilleke, Performance of a compact spiral coil heat exchange. *Heat Recovery Syst. and CHP*, 15(5): p. 457–468, 1995.
4. Lee, M., Kang, T. and Y. Kim, Air-side heat transfer characteristics of spiral-type circular fin-tube heat exchangers, *international journal of refrigeration*, 33(2): p. 313–320, 2010.
5. Mittal, M.K., Kumar, R. and A. Gupta, Numerical analysis of adiabatic flow of refrigerant through a spiral capillary tube, *International Journal of Thermal Sciences*, 48(7): p. 1348–1354, 2009.
6. Nakayama, A., Kokubo, N., Ishida, T., and F. Kuwahara, Conjugate numerical model for cooling a fluid flowing through a spiral coil immersed in a chilled water container, *Numer. Heat Transfer: Part A*, 37(2): p. 155–165, 2000.
7. Naphon, P., and J. Suwagrai, Effect of curvature ratios on the heat transfer and flow developments in the horizontal spirally coiled tubes, *International Journal of Heat and Mass Transfer*, 50(3): p. 444–451, 2007.
8. Naphon, P., and S. Wongwises, An experimental study on the in-tube heat transfer coefficients in a spiral-coil heat exchanger, *International Communications in Heat and Mass Transfer*, 29(6): p. 797–809, 2002.
9. Naphon, P., and S. Wongwises, A study of the heat transfer characteristics of a compact spiral coil heat exchanger under wet-surface conditions, *Experimental Thermal and Fluid Science*, 29(4): p. 511–521, 2005.
10. Naphon, P., and S. Wongwises, Investigation of the performance of a spiral-coil finned tube heat exchanger under dehumidifying conditions, *Journal of Engineering Physics and Thermophysics*, 76(1): p. 83–92, 2003.
11. Oliveira, P.J., and R.I. Issa, An Improved PISO Algorithm for the Computation of Buoyancy-Driven Flows, *Numerical Heat Transfer*, 40(6): p. 473–493, 2001.
12. Orlov, V.K., and P.A. Tselishchev, Heat exchange in spiral coil with turbulent flow of water. *Thermal Engineering*. (Translated from *Teploenergetika*), 11(12): p. 97–99, 1964.
13. Ramana Rao, M.V., and D. Sadasivudu, Pressure drop studies in helical coils, *Indian journal of technology*, 12(1): p. 473–479, 1974.
14. Seyedashraf, O., and A.A. Akhtari, Flow separation control in open-channel bends, *Journal of the Chinese Institute of Engineers*, 39(1): p.40–48, 2016.

15. Shaukat, A., Pressure drop correlations for flow through regular helical coil tubes, *J. Fluid Dynamic Research*, 28(4): p. 295-310, 2001.
16. Shaukat, A., and C.V. Seshadri, Pressure drop in Archimedean spiral tubes, *Industrial & Engineering Chemistry Process Design and Development*, 10(3): p. 328–332, 1971.
17. Shaukat, A., and A.H. Zaidi, Head loss and Critical Reynolds Numbers for Flow in ascending equiangular spiral tube coils, *Industrial & Engineering Chemistry Process Design and Development*, 18(2): p. 349–353, 1979.
18. Srinivasan, P.S., Nandapurkar, S.S. and F.A. Holland, Pressure drop and heat transfer in coils, *Transactions of the institution of chemical engineering and the chemical engineer*, 46(4), 1968.
19. Van Leer, B., MUSCL, A New Approach to Numerical Gas Dynamics, in *Computing in Plasma-physics and Astrophysics*, in *Proceedings of the Second European Conference on Computational Physics*. Max-Planck-Institut für Plasmaphysik, Garching, 1976.
20. Versteeg, H.K., and W. Malalasekera, *Computational Fluid Dynamics*, Longman Group, (1995).
21. Yoo, G. J., Choi, H. K., and W.R. Dong, Fluid flow and heat transfer characteristics of spiral coiled tube: Effects of Reynolds number and curvature ratio, *Journal of Central South University*, 19(2): p. 471–476, 2012.